

3-DIMENSIONAL NUMERICAL STUDIES TO EVALUATE THE EFFECT OF INFILL MATERIALS ON THE PERFORMANCE OF GEOCELL REINFORCED SOFT CLAY BEDS

A.Hegde and T.G.Sitharam, Department of Civil Engineering, Indian Institute of Science, Bangalore, India, 560012

ABSTRACT

Nowadays, the geocell are being widely used to strengthen the soft soil. This study intends to quantify the effect of infill materials on the performance of the geocell reinforced soft clay beds with the help of 3-dimensional numerical simulations. Sand, aggregates, and the silty clay were the three different infill materials used in the present study. Numerical simulations were carried out using FLAC^{3D} considering its ability to model the complex geotechnical problems. The foundation soil, infill soil and the geocell materials were simulated with three different material models, namely, modified Cam-clay, Mohr Coulomb and the linear elastic. The actual honeycomb shape of the geocell was modeled in FLAC^{3D} using the digitization technique. Firstly, the numerical model was validated with the published experimental results. Using the validated numerical model, the effects of different infill materials were studied. Out of three infill materials studied, aggregates were found to be most beneficial in increasing the performance of geocell reinforced soft clay beds. The bearing capacity of the soft clay bed was increased by more than five times in case of all the infill material. Irrespective of the type infill material used, geocells found to distribute the load in lateral direction.

1. INTRODUCTION

Geocells are the cost effective, sustainable construction materials used to enhance the performance of soft soil. These are three-dimensional in shape and are made up of ultrasonically welded high strength polymers or the polymeric alloy such as Polyethylene, Polyolefin etc. Geocells are being widely used in geotechnical engineering for stabilization and protection applications. Due to its 3-dimensional structure, it offers all-round confinement to the encapsulated soil, which leads to the overall improvement in the performance of the foundation bed. In recent years, many researchers have studied the beneficial aspects of the cellular reinforcement through laboratory model plate load tests (Yang et al., 2012; Thakur et al., 2012; Tanyu et al., 2013; Hegde and Sitharam, 2014a; Hegde et al.2014).

One important aspect of the geocell, which is not fully understood, is the effect of the infill materials on its performance. Generally, sand or fine granular fill (i.e. compactable materials) are used to fill the geocell pockets. Han et al. (2010) conducted the laboratory model tests on a single geocell with three different infill materials viz. poorly graded river sand, quarry waste (stone chips) and well graded aggregate. It was found that the geocell with sand infill was performed better under the static loads, while the geocell filled with aggregate was found effective under the action of dynamic loads. Lambert et al. (2011) used the mixture of the sand and scrap tire to fill the geocell

pockets and noted that the characteristics of the fill material largely affects the response of the geocell to the uniaxial compression loading. Hegde and Sitharam (2014b) reported that the performance of the geocell reinforced soft clay bed increases with the increase in the friction angle of the infill materials.

In the present study, the effect of infill materials on the performance of the geocell has been studied with the help of 3D numerical studies. Crushed aggregate, silty clay and sand were the three different infill materials used in the investigation. A biaxial geogrid layer was also placed at the base of the geocell in all the reinforced tests. In the remaining part of the manuscript, the term 'geocell reinforcement' indicates the combination of geocell and the basal geogrid. The numerical model was validated with the results of the laboratory model studies reported by Hegde and Sitharam (2013). The laboratory test results of the two cases, namely, unreinforced and the geocell with sand infill cases were used for the validation of the numerical model.

The first part of the manuscript deals with the modeling procedure and the validation aspects; whereas the second part deals with the results of the numerical studies. For convenience, the size of the numerical model was maintained same as that of size of the test bed used by Hegde and Sitharam (2013).

2. NUMERICAL ANALYSIS

2.1 Model Details

In the present study, FLAC^{3D} was chosen for the analysis considering its ability to model a wide range of geotechnical problems. The dimension of the model was 0.9 m x 0.9 m x 0.6 m. The schematic view of the test setup as reported by Hegde and Sitharam (2013) has been shown in Figure 1. The modified Cam-clay model was used to simulate the behavior of the soft clay bed and the Mohr Coulomb model was used to simulate the behavior of the different infill materials. The geocell was modelled using the geogrid structural element. The geogrid structural elements can resist the membrane stresses but cannot resist the bending stresses. The rigid nature of the geocell joint was simulated by fixing the nodes representing the joints. Linear elastic model was used to simulate the behavior of the geocell.

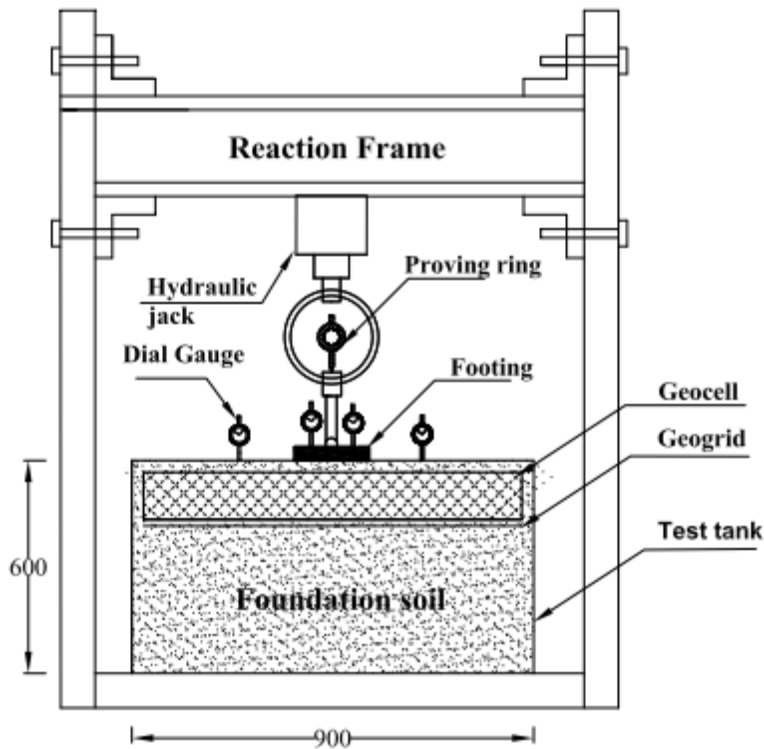


Figure 1. Schematic view of the test set-up

The interfaces between the geocell and the soil were linearly modelled with Mohr Coulomb yield criterion. Only quarter portion of the test bed was modelled using symmetry to reduce the computational effort. The quarter symmetric model of size 0.45 m x 0.45 m x 0.6 m was discretized into 9216 zones. Analyses were carried out under controlled velocity of magnitude of 2.5×10^{-5} m/step. The displacement along the bottom boundary (which represents tank bottom) was restrained in both horizontal as well as vertical directions. The side boundaries (which represent tank side) were restrained only in the horizontal direction, such that the displacements were allowed to occur in the vertical direction. By providing the lateral resistance to the soil nodes representing the area of the footing, roughness of the footing was simulated. Similar to the laboratory studies, the undrained test condition was maintained during the modelling process.

2.2 Determination of Model Parameters

An isotropic triaxial compression test was conducted to determine the Cam-clay parameters, λ (slope of the normal consolidation line) and κ (slope of the swelling line) and p'_c (pre-consolidation pressure). Figure 2a shows the relationship between specific volume (v) and natural logarithmic of mean effective stress ($\ln p'$). The isotropic triaxial

compression test was carried out in three cycles, i.e. loading, unloading and reloading. During the loading cycle, the sample was consolidated under 7 different confining pressures from 50 kPa to 350 kPa with an increment of 50 kPa in each step. At 100 kPa, the change in the slope of the line was observed, indicating the particular value of the pressure is nothing but the pre-consolidation pressure. During unloading, the pressure was reduced from 350 kPa to 50 kPa in 7 steps with the decrement of 50 kPa in each step. In the reloading cycle, the confining pressure was increased to 450 kPa in 8 steps. The parameter M (slope of the critical state line) and elastic modulus of the clay were determined from the consolidated undrained triaxial compression test. The test was carried out at three different confining pressures of 100 kPa, 200 kPa and 300 kPa. Figure 2b shows the critical state line determined from the CU triaxial test. Table 1 represents properties of different materials used in the numerical simulations.

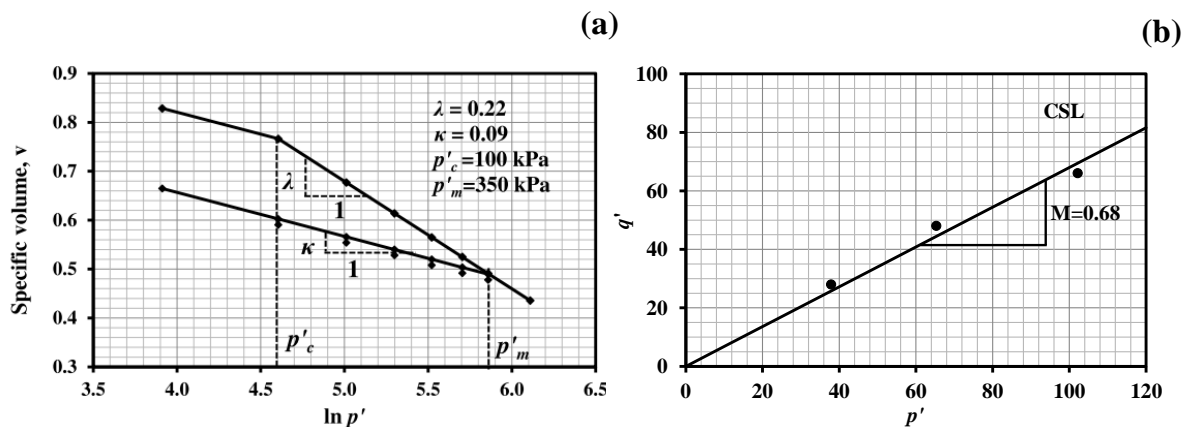


Figure 2a-b. Cam-clay parameters: (a) v vs. $\ln p'$; (b) critical state line

The shear strength properties of the sand and clay were obtained from the direct shear test and the undrained triaxial compression test respectively. However, the shear strength properties of the aggregates were taken from the box shear test results provided by the supplier. The properties of the different infill materials are summarized in the Table 2. The elastic modulus of the sand and the silty clay were determined from the consolidated undrained triaxial compression test. Initial tangent modulus was determined from the stress-strain curve corresponding the confining pressure of 200 kPa. The aggregate used in the experiment was relatively softer in nature. Crushing of the aggregates was observed during the experiments at higher loads. Hence, elastic modulus value similar to soft weathered rock was chosen for the aggregates. The elastic modulus of the geocell and geogrid was determined from tensile stress-strain behavior shown in Figure 3. The secant modulus was determined corresponding to 2% axial strain in both the cases. The interface shear strength properties (c_i and ϕ_i) for both geocell and geogrids were obtained from the modified direct shear test. The interface shear modulus value (k_i) of 2.36 MPa/m was considered in the analysis for geocells and geogrids (Itasca, 2008).

Table 1. Properties of different materials used in numerical modelling

Parameters	Values
Clay	
Shear modulus, G (MPa)	1.36
Friction constant, M	0.68
Slope of NCL, λ	0.22
Slope of swelling line, κ	0.09
Specific volume at reference pressure, v_{λ}	1.78
Pre-consolidation pressure, p'_c	100
Unit weight, γ (kN/m ³)	20
Geocells	
Young's modulus, E (MPa)	275
Poisson's ratio, μ	0.45
Interface shear modulus, k_i (MPa/m)	2.36
Interface cohesion, c_i (kPa)	0
Interface friction angle, ϕ_i (°)	30
Thickness, t_i (mm)	1.5
Geogrids	
Young's modulus, E (MPa)	210
Poisson's ratio, μ	0.33
Interface shear modulus, k_i (MPa/m)	2.36
Interface cohesion, c_i (kPa)	0
Interface friction angle, ϕ_i (°)	18
Thickness, t_i (mm)	1.5

Table 2. Properties of different infill materials

Properties	Silty clay	Sand	Aggregate
Friction angle, ϕ (°)	27	35	40
Cohesion, c (kPa)	20	0	0
Bulk modulus, K (MPa)	5	6	7.2
Shear Modulus, G (MPa)	2.3	2.9	3.3
Poisson's ratio, μ	0.3	0.3	0.3

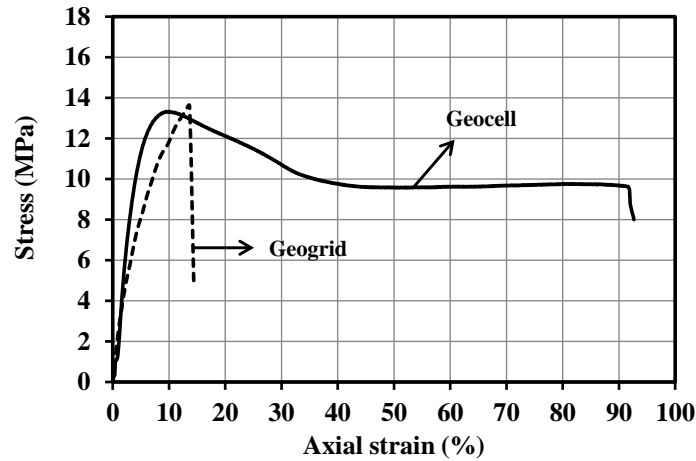


Figure 3. Tensile stress-strain behavior of geocell and geogrid

Preliminary analyses carried out revealed that the boundary distances did not influence the results as deformations and stresses were contained within the boundaries. It is understood that the geocell is made of multiple interconnected cells and the shape of each such cell is same. Hence, a photograph of the single cell was taken and it was digitized to obtain the actual curvature of the cell. The co-ordinates were deduced from the curvature and the same were used in the FLAC^{3D} to model the actual shape of the geocell. Figure 4a-b shows the FLAC^{3D} models of the different cases considered in the study.

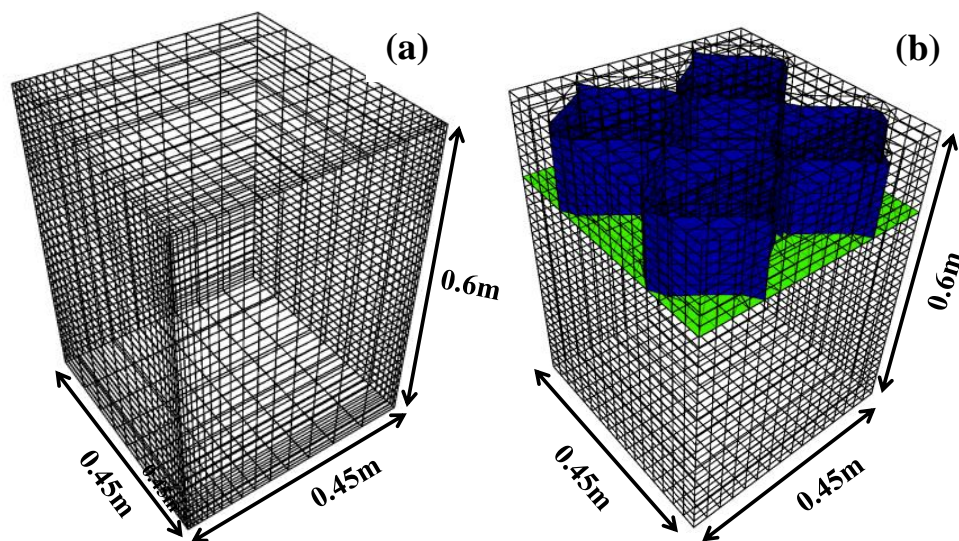


Figure 4a-b. FLAC^{3D} model for different cases: (a) unreinforced; (b) geocell and geogrid reinforced

3. RESULTS AND DISCUSSION

Firstly, the numerical model was validated with the results of laboratory model plate load test reported by Hegde and Sitharam (2013). Only two cases were compared for the validation i.e. unreinforced and the geocell with sand infill material. Figure 5 shows the comparison of experimental and numerical bearing pressure-settlement response. There exists a good agreement between the experimental and numerical results. Clearly defined failure was observed in case of the unreinforced clay bed. The slope of the pressure settlement curve becomes nearly vertical beyond $S/B= 5\%$, indicating the failure of the foundation. No clear-cut failure was observed in case of the geocell reinforced clay beds with sand infill up to a large settlement of $S/B=45\%$. . Geocells found to take up the footing loads even after the failure of the foundation bed.

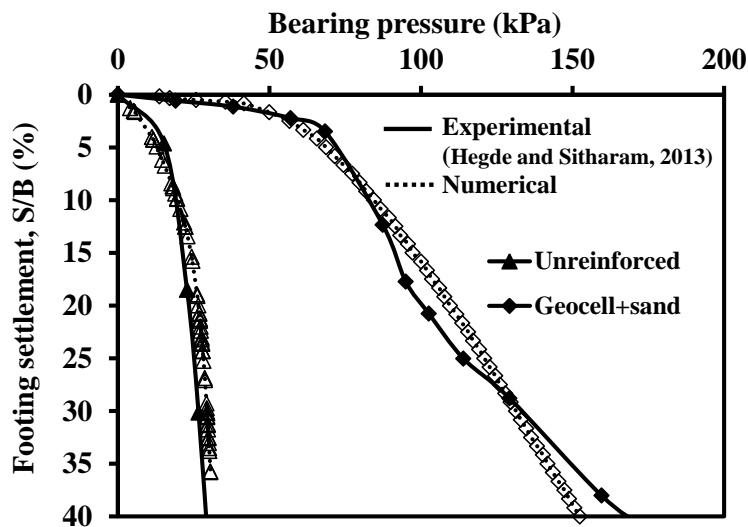


Figure 5. Comparison of experimental and numerical pressure-settlement behavior

Using the validated numerical model, the performance of the different infill materials was evaluated. Figure 6 shows the numerically obtained pressure-settlement behaviors for different cases. Out of three different infill materials, the maximum bearing capacity was observed in the case of aggregate infill materials. The inner surface of the geocell is made up of unique textures. When infill material comes in contact with these textures, friction force will be developed between the material and the geocell inner surface. The friction force, thus originated not only resists the imposed load, but also helps to increase the bearing capacity of the reinforced clay beds. The friction force also ensures the bonding between geocell and the infill material matrix. More is the friction angle better is the load carrying capacity. The aggregates possess higher friction angle compared red soil and the sand and also the better interlocking properties. Interlocked aggregates form the composite mass with the geocell, which acts as a rigid slab to resist the load, conceding the minimal footing settlement. However, not much difference was observed in the performances of different infill materials.

The increase in the bearing capacity due to the provision of the reinforcement can be quantified through a non-dimensional parameter called bearing capacity improvement factor (I_f), which is defined as,

$$I_f = \frac{q_r}{q_o} \tag{1}$$

Where q_r is the bearing pressure of the reinforced bed at a particular settlement and q_o is the bearing pressure of unreinforced bed at the same settlement. Bearing capacity improvement factor is similar to the bearing capacity ratio, reported by Binquet and Lee (1975). When the ratio is beyond the ultimate bearing capacity of the unreinforced bed, the ultimate bearing capacity (q_{ult}) is used instead of q_o . Figure 7 represents the variation of the bearing capacity improvement factors with the footing settlement for different infill materials. The bearing capacity improvement factors found to vary between 4 and 5.5. For example, $I_f=5.5$ indicates the 5.5 times higher bearing capacity in case of the geocell reinforced clay bed as compared to unreinforced bed.

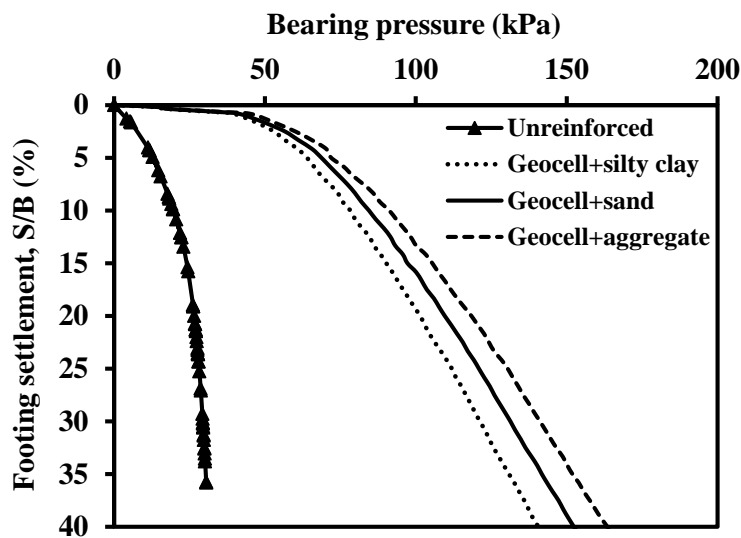


Figure. 6 Pressure-settlement behavior for different infill soils

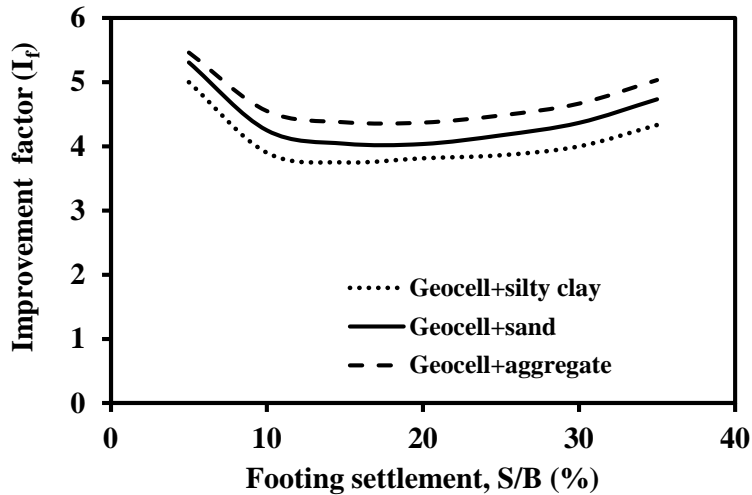


Figure 7. Bearing capacity improvement factors (I_f) for different infill materials

The performance improvement of the foundation bed due to geocell reinforcement can also be quantified in terms of the reduction in the settlement of the footing using the parameter called percentage reduction in settlement (PRS). PRS is defined as,

$$PRS = \left(\frac{S_o - S_r}{S_o} \right) \times 100 \quad (2)$$

where S_o is settlement of the unreinforced foundation bed corresponding to its ultimate bearing capacity. The double tangent method (Vesic, 1973) was used to estimate the ultimate load bearing capacity. According to this method the ultimate bearing capacity is defined as the pressure corresponding to the intersection of the two tangents; one at the early part of the pressure settlement curve and the another at the latter part. In the present case, the ultimate bearing capacity was found out to be 5% of the footing width ($S/B=5\%$). S_r is settlement of reinforced foundation bed corresponding to the footing pressure equal to the ultimate bearing pressure of unreinforced foundation bed. Figure 8 shows the PRS values for different infill materials. The PRS values found to vary between 91% and 94% for different infill materials. Maximum PRS value of 94% was observed in case of the aggregate infill. PRS=94% indicates the 94% reduction in the settlement in the geocell reinforced case as compared to unreinforced bed.

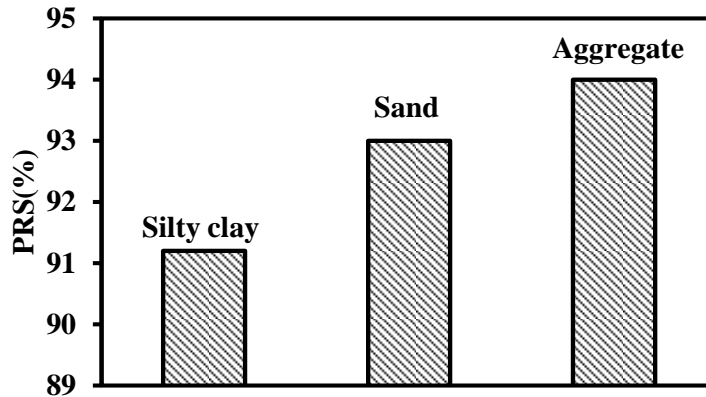


Figure 8. PRS values for different infill materials

Figure 9 shows the typical vertical stress contours for unreinforced case and the geocell with sand infill materials. The reported stress contours are corresponding to the applied vertical stress equal to the ultimate bearing capacity of the unreinforced soft clay bed. The distribution of the stress contours indicates that the tank boundaries have no bearing on the results. Uniform distribution of the stresses up to the large depth was observed in case of the unreinforced bed. In case of the geocell reinforced case, the influence depth of the stress was reduced as compared to the unreinforced bed. Irrespective of the infill materials used, the geocells found to distribute the load in lateral direction. Similar type of observations was also made by Hegde and Sitharam (2015a, b). The interconnected cells form a panel that acts like a large mat that transfers the imposed load to the larger area, leading to better performance of the foundation beds. This mechanism is known as beam mechanism.

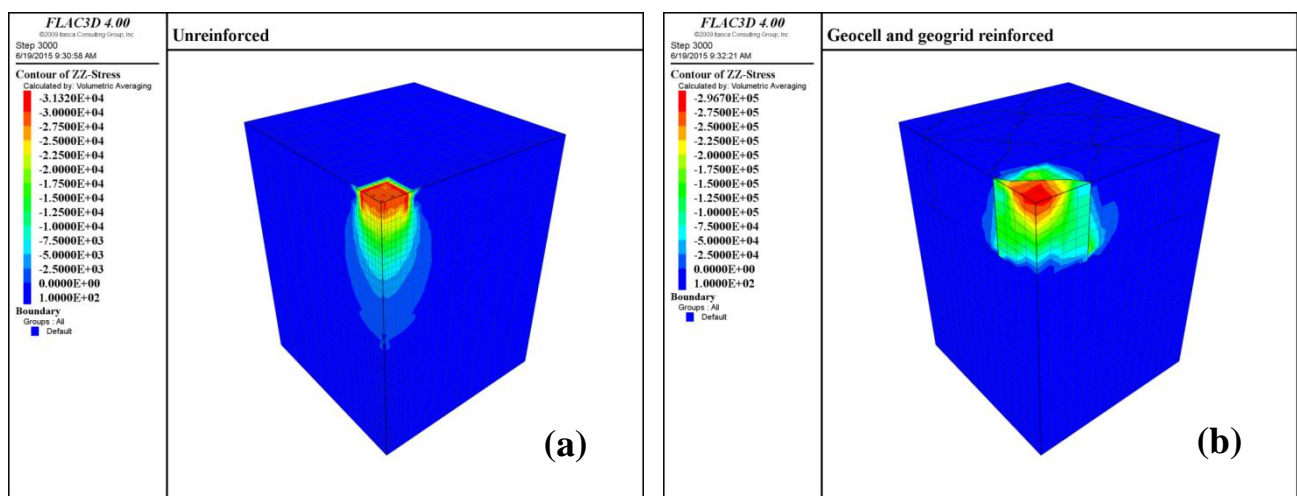


Figure 9a-b. Vertical stress contours (N/m²): (a) unreinforced; (b) geocell with sand infill

4. CONCLUSIONS

This paper presents the results of the 3D numerical studies conducted on the geocell reinforced soft clay beds. The geocell pockets were filled up with three different infill materials, namely, silty clay, sand and the aggregates. Initially, the model was calibrated with the experimental studies. The bearing capacity of the foundation bed was increased by more than 5 times in the presence of geocells for all the infill materials. Similarly, the settlement of the foundation bed was reduced by more than 90% in the presence of geocells. Out of three different infill materials used in the study, the performance of the aggregates was found to be more effective. With the increase in the friction angle of the infill material, the performance of the geocell reinforced soft clay bed was increased. Further, the geocells found to distribute the load in the lateral direction irrespective of the infill materials being used.

Even though, aggregates were found to be beneficial, the overall performance of the soft clay bed was not varied much with other infill materials. Locally available soil with sufficient amount of silt or fine sand content can also be used at sites to fill the geocell pockets. In general, it can be concluded that the effect of infill material on the performance of the geocell is marginal and it should be left to the site engineers to choose the suitable infill material as per the prevailing of the site condition.

REFERENCES

- Binquet, J., and Lee, L. K. (1975). Bearing capacity tests on reinforced earth slabs. *Journal of Geotechnical Engineering*, 101(12): 1241–1255.
- Han, J., Pokhrel, S.K., Parsons, R.L., Leshchinsky, D. and Halahmi, I. (2010). Effect of infill material on the performance of geocell-reinforced bases. *Proceedings of 9th International Conference on Geosynthetics*, Brazil, 1503-1506.
- Hegde, A., and Sitharam, T. G. (2013). Experimental and numerical studies on footings supported on geocell reinforced sand and clay beds. *International Journal of Geotechnical Engineering*, 7(4): 347-354.
- Hegde, A., and Sitharam, T. G. (2014a). Joint strength and wall deformation characteristics of a single cell subjected to uniaxial compression. *International Journal of Geomechanics*. DOI: 10.1061/(ASCE)GM.5622.0000433.
- Hegde, A. M., and Sitharam, T. G. (2014b). Effect of infill materials on the performance of geocell reinforced soft clay beds. *Geomechanics and Geoengineering*. DOI: 10.1080/17486025.2014.921334
- Hegde, A., and Sitharam, T. G. (2015a). 3-Dimensional numerical modelling of geocell reinforced sand beds. *Geotextiles and Geomembranes*, DOI:10.1016/j.geotextmem.2014.11.009.
- Hegde, A.M. and Sitharam, T.G. (2015b). 3-Dimensional numerical analysis of geocell reinforced soft clay beds by considering the actual geometry of geocell pockets. *Canadian Geotechnical Journal*, DOI: 10.1139/cgj-2014-0387
- Hegde, A., Kadabnakatti, S. and Sitharam, T.G. (2014). Protection of buried pipelines using a combination of geocell and geogrid reinforcement: experimental studies. *Geotechnical Special Publication, ASCE*, 238: 289-298.
- Itasca. (2008). Fast Lagrangian Analysis of Continua (FLAC3D 4.00). Itasca Consulting Group Inc, Minneapolis, USA.



- Lambert, S., Nicot, F. and Gotteland, P. (2011). Uniaxial Compressive behavior of scrapped tire and sand filled wire netted geocell with a geotextile envelop. *Geotextiles and Geomembranes*, 29: 483-490.
- Tanyu, B. F., Aydilek, A. H., Lau, A. W., Edil, T. B. and Benson, C. H. (2013). Laboratory evaluation of geocell-reinforced gravel sub-base over poor subgrades. *Geosynthetics International*, 20 (2): 46-71.
- Thakur, J. K., Han, J., Pokharel, S. K. and Parsons, R. L. (2012). Performance of geocell-reinforced recycled asphalt pavement (RAP) bases over weak subgrade under cyclic plate loading. *Geotextiles and Geomembranes*, 35: 14-24.
- Vesic, A.S., (1973). Analysis of ultimate loads of shallow foundations. *Journal of Soil Mechanics and Foundation Division*. ASCE, 99 (SM1), 45-69
- Yang, X., Han, J., Pokharel, S.K., Manandhar, C., Parsons, R.L., Leshchinsky, D. and Halahmi, I., (2012). Accelerated pavement testing of unpaved roads with geocell reinforced sand bases. *Geotextiles and Geomembranes*, 32: 95-103.